FINAL REPORT

Enhancement of TEM Data and Noise Characterization by Principal Component Analysis

SERDP Project MM-1640

MAY 2010

M. Andy Kass, Yaoguo Li,
Richard Krahenbuhl,
Misac Nabighian
Center for Gravity, Electrical, & Magnetic Studies
Department of Geophysics
Colorado School of Mines

Douglas Oldenburg
University of British Columbia
Geophysical Inversion Facility

This document has been approved for public release.

DoD EPA DOE SERDP
Strategic Environmental Research and Development Program

Report Documentation Page

Form Approved
OMB No. 0704-0188

Public reporting burden for the collection of information is estimated to average 1 hour per response, including the time for reviewing instructions, searching existing data sources, gathering and maintaining the data needed, and completing and reviewing the collection of information. Send comments regarding this burden estimate or any other aspect of this collection of information, including suggestions for reducing this burden, to Washington Headquarters Services, Directorate for Information Operations and Reports, 1215 Jefferson Davis Highway, Suite 1204, Arlington VA 22202-4302. Respondents should be aware that notwithstanding any other provision of law, no person shall be subject to a penalty for failing to comply with a collection of information if it does not display a currently valid OMB control number.

1. REPORT DATE	2. REPORT TYPE	3. DATES COVERED
MAY 2010		**00-00-2010 to 00-00-2010**

4. TITLE AND SUBTITLE	5a. CONTRACT NUMBER
Enhancement of TEM Data and Noise Characterization by Principal Component Analysis	5b. GRANT NUMBER
	5c. PROGRAM ELEMENT NUMBER
6. AUTHOR(S)	5d. PROJECT NUMBER
	5e. TASK NUMBER
	5f. WORK UNIT NUMBER
7. PERFORMING ORGANIZATION NAME(S) AND ADDRESS(ES) **Colorado School of Mines,Department of Geophysics,Center for Gravity, Electrical, & Magnetic Studies,Golden,CO,80401**	8. PERFORMING ORGANIZATION REPORT NUMBER
9. SPONSORING/MONITORING AGENCY NAME(S) AND ADDRESS(ES)	10. SPONSOR/MONITOR'S ACRONYM(S)
	11. SPONSOR/MONITOR'S REPORT NUMBER(S)

12. DISTRIBUTION/AVAILABILITY STATEMENT
Approved for public release; distribution unlimited

13. SUPPLEMENTARY NOTES

14. ABSTRACT

15. SUBJECT TERMS

16. SECURITY CLASSIFICATION OF:			17. LIMITATION OF ABSTRACT	18. NUMBER OF PAGES	19a. NAME OF RESPONSIBLE PERSON
a. REPORT **unclassified**	b. ABSTRACT **unclassified**	c. THIS PAGE **unclassified**	**Same as Report (SAR)**	**61**	

This report was prepared under contract to the Department of Defense Strategic Environmental Research and Development Program (SERDP). The publication of this report does not indicate endorsement by the Department of Defense, nor should the contents be construed as reflecting the official policy or position of the Department of Defense. Reference herein to any specific commercial product, process, or service by trade name, trademark, manufacturer, or otherwise, does not necessarily constitute or imply its endorsement, recommendation, or favoring by the Department of Defense.

Enhancement of TEM Data and Noise Characterization by Principal Component Analysis

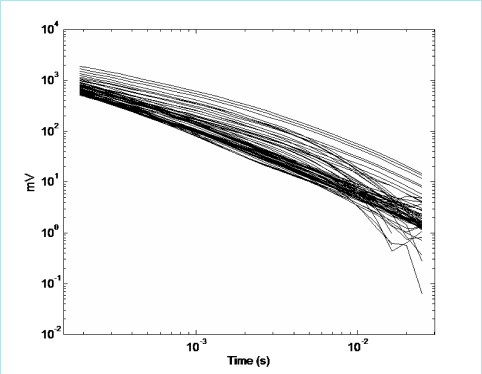

Removing viscous remanent magnetization from TEM data at Kaho'olawe, HI

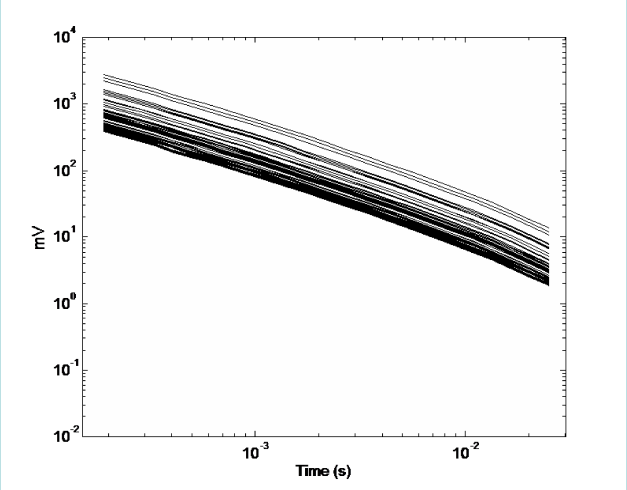

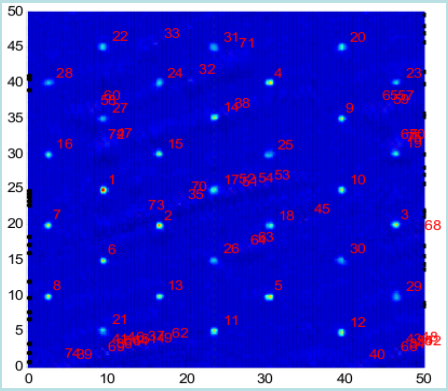

Reducing false picks due to sensor movement

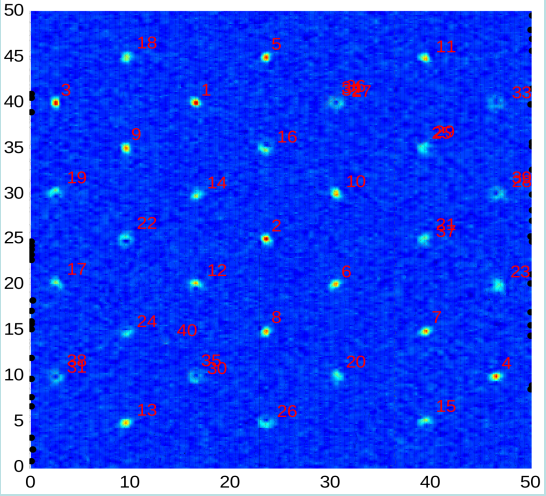

Final Report

SERDP SEED Project MM-1640

M. Andy Kass, Yaoguo Li, Richard Krahenbuhl, Misac Nabighian
Center for Gravity, Electrical, & Magnetic Studies
Department of Geophysics
Colorado School of Mines

Douglas Oldenburg
University of British Columbia
Geophysical Inversion Facility

May 2010

SERDP
Strategic Environmental Research and Development Program

EXECUTIVE SUMMARY

This is the final report for the SERDP project MM-1640 and it covers the research results accomplished since the inception of the project in 2007. The basic premise of this project is the theoretical understanding and algorithm development of principal component analysis (PCA) as a de-noising and signal-separation tool for transient electromagnetic (TEM) data in unexploded ordnance (UXO) applications. There is an express need for techniques to reduce the presence of random noise in TEM data as well as reduce the influence of correlated noise due to a wide variety of sources on automatic anomaly-picking routines for more accurate detection with fewer false anomalies. We have developed an algorithm and workflow for the processing and inversion of TEM data that attenuates signal from undesired sources and accurately inverts TEM data for diagnostic UXO parameters.

The research performed over the life-span of this project has progressed satisfactorily with the major research tasks completed approximately to project plan. In addition, we have identified an additional area of research critical to the application of PCA to TEM data and added these aspects to the research plan.

First, we developed a principal component analysis algorithm tailored to unexploded ordnance applications. Decay characteristics of TEM data preclude the standard Karhunen-Loéve transform; we have addressed these issues with algorithm modifications and incorporated these into the workflow.

Secondly, we identified the optimum choice of principal components for the attenuation of both random noise and correlated noise, leaving the signal due to UXO intact. We show that the processed data is optimally prepared for automatic anomaly picking routines with a highly reduced number of false anomalies. We demonstrate this on both synthetic examples of UXO surveys, as well as on TEM data from Kaho'olawe, Hawaii, USA.

Finally, we have identified a critical issue with inversion of processed data that results in extremely inaccurate recovered models without the incorporation of the PCA process into the forward model. We developed an inversion algorithm which takes the processing steps into account during construction of the inverse kernels. This leads to more accurate recovered models of inverted anomalies.

TABLE OF CONTENTS

EXECUTIVE SUMMARY iii

LIST OF FIGURES vii

LIST OF TABLES ix

LIST OF ACRONYMS xi

CHAPTER 1 INTRODUCTION 1

1.1 SERDP relevance 1
1.2 Technical objectives 3
1.3 Project summary 4

CHAPTER 2 BACKGROUND 5

2.1 Principal component analysis 5

CHAPTER 3 ALGORITHM DEVELOPMENT 11

3.1 Introduction 11
3.2 Principal component analysis for transient electromagnetic surveys . . 12
3.2.1 Temporal correlation 12
3.3 Removal of uncorrelated noise 15
3.4 Removal of correlated noise 16
3.5 Spatial correlation 16
3.6 Large-scale decompositions 17
3.6.1 Iterative eigenvalue decompositions 18
3.7 Anomaly selection 19
3.8 Inversion of processed data 19
3.9 Algorithm summary 23

CHAPTER 4 RESULTS 25

4.1 Uncorrelated noise removal 25
4.2 Inversion of processed data 28
4.2.1 Linear inversion 28
4.2.2 Non-linear inversion 29
4.3 Correlated noise removal 32

CHAPTER 5 SUMMARY 39

REFERENCES CITED 45

APPENDIX A PUBLICATIONS AND PRESENTATIONS 47

LIST OF FIGURES

3.1 General workflow for processing TEM data with principal component analysis 12

3.2 Covariance calculations (a) before and (b) after normalization of the data. 14

4.1 First time gate of EM63 data collected over the Kaho'olawe Navy QA grid. Note the large geologic response due to viscous remnant magnetization (VRM). 26

4.2 (a) 65 example decay curves from Kaho'olawe. Some traces include responses from unexploded ordnance; these traces deviate from the expected t^{-1} decay. (b) Geologic response constructed with only the first principal component. The curve exhibits the expected inverse power law decay due to horizontal layering and magnetic soils. (c) TEM decay curves constructed with the first and second principal components. The (approximate) superposition of UXO signal on the geologic signal is clear, with significant reduction of random noise in later channels. (Negative values not displayed) 27

4.3 Original and recovered model (a) through smallest model solution, (b) after PCA on data only, and (c) after PCA on data and kernels. . . . 30

4.4 L-curve for (a) original inversion, (b) inversion with rotated data, and (c) inversion with rotated data and rotated sensitivity matrix. 31

4.5 Effect of cart orientation error in a UXO survey. Orientation error produces an approximate 50 mV response in this example, visible in the approximate east/west lineations. 33

4.6 Radially averaged power spectrum of the original data set, orientation error, and UXO signal. The difference between the power spectra of the orientation error and the UXO signal indicates that they are inseparable in the frequency domain. 34

4.7 Three different examples of Butterworth filtering. The filtering is unable to separate the cart orientation error and UXO for a variety of cutoff wavenumbers. 35

4.8 UXOLab target picks in a dataset contaminated with orientation error. Note the large number of picks corresponding to the cart orientation error (linear bands of picks). The dashed line corresponds to transects shown in Figure 4.9. 36

4.9 Example lines from one time gate before and after PCA. Units in mV. (a) Line including both UXO anomalies as well as cart orientation error. (b) Same line after PCA. Choosing a threshold from this line (8 mV) produced better anomaly picking results than from the non-PCA line. The numbers assigned to each peak are assigned by the autopicking routine, and thus change before and after PCA. (c) Example line that contains no UXO anomalies. Note the large anomaly due to orientation error. (d) Same line after PCA. No appreciable structure is present, and the magnitude is well below that of the UXO anomalies. 37

4.10 UXOLab anomaly picks after processing with PCA. After clustering, there was one false anomaly and no missed targets. 38

LIST OF TABLES

3.1 Recommended PCA algorithm. Numbers in parentheses correspond to sections with detailed descriptions. 23

4.1 Nonlinear inversion results. Only by applying PCA to both the data and the kernels were we able to properly recover diagnostic parameters. 32

LIST OF ACRONYMS

AEM - Airborne Electromagnetic

GCV - Generalized Cross Validation

m - meter

mV - millivolt

PCA - Principal Component Analysis

RF - Radio Frequency

RGB - Red/Green/Blue

SERDP - Strategic Environmental Research and Development Program

TEM - Transient Electromagnetic

UXO - Unexploded Ordnance

VRM - Viscous Remnant Magnetization

CHAPTER 1
INTRODUCTION

1.1 SERDP relevance

This project addresses the need for improved signal processing outlined in the Statement of Needs MMSEED-08-01, and has developed new technologies for enhancing time-domain electromagnetic data (TEM) by estimating and removing undesirable components such as random noise and other responses unrelated to metallic objects. The goal is to increase the signal-to-noise ratio of the TEM data as well as to generate an estimate of data noise characteristics (statistical distribution and associated parameters) for use in subsequent inversion-based discrimination.

One of the most effective geophysical techniques for UXO application is the transient electromagnetic method. Using a loop as a source, a time-varying magnetic field is generated at the surface which in turn induces electrical currents in the ground, and more importantly in buried metallic objects. Once induced, these currents dissipate over time due to ohmic losses, leading to a measured transient decay in magnetic field flux density at the surface by geophysical sensors. The currents induced in the surrounding medium and in the buried metallic objects decay at different rates and can be separated. For metallic objects, the decay rates are directly related to the size, shape, depth, and electrical conductivity of the target body. Unfortunately, real TEM data for UXO detection and discrimination are contaminated with outside noise sources. These sources of noise can be spatially correlated, such as near-surface geology, micro-topography, coil orientation, sensor motion, and positioning errors; or they can be uncorrelated, such as random RF interference, telluric sources, and instrument interference. Each of these sources of noise, in addition to buried UXO, contributes to the total response measured by the sensors. The effect of noise is especially strong at late-times in the TEM data. Noise from such numerous and varying sources often

limits the ability of the TEM method to adequately discriminate hazardous munitions from non-hazardous items. Thus, there is a need for developing methods to enhance TEM data in UXO discrimination, and the key to the solution under such conditions is to develop a practical algorithm that can reliably identify and remove these individual sources of noise component by component.

Of the two types of noise, correlated noise is more difficult to isolate and remove from the data than uncorrelated noise. Current methods of noise analysis in UXO surveys include simply thresholding a noise level and ignoring any signal below the chosen value (Pasion and Oldenburg, 2001b), stacking, and median filters to de-trend the data (Pasion and Oldenburg, 2001a). To date, there has not been a concentrated research effort focused on separating the various sources of noise, and identifying the effects that these individual sources have on the data.

Principal component analysis, or PCA, is a technique for simplifying a data set by reducing multidimensional data sets to lower dimensions for analysis. PCA is basically an orthogonal linear transformation that transforms the data to a new coordinate system such that the greatest variance by any projection of the data comes to lie on the first coordinate (called the first principal component), the second greatest variance on the second coordinate, and so on. By properly analyzing the various components, one can isolate the individual correlated signals not associated with the UXO, and remove those components from the TEM data. In an ideal case, this leaves only the signal from UXO and UXO-like anomalies, eliminating completely any error in the signal caused by external noise.

We have developed a set of processing techniques based on the PCA algorithm for TEM data in UXO applications as well as the parametric inversion of such processed data for recovering both extrinsic and intrinsic parameters for use in discrimination. These techniques can be combined with existing workflows to rapidly identify potential UXO targets for further processing with minimal required user input.

1.2 Technical objectives

The purpose of this study was to develop a practical algorithm that enhances the signal in transient electromagnetic data for UXO applications. We have developed a de-noising algorithm that not only removes random, uncorrelated noise, but also separates the signals due to various sources through principal component analysis. We separated the research into aspects of PCA that address uncorrelated signals and aspects that address correlated but undesired signals. Specifically, this study had six objectives in three categories:

- Method development for uncorrelated noise
  - Develop a PCA algorithm tailored to TEM data from UXO surveys, and
  - Produce a stable and automated algorithm for removal of uncorrelated noise.
- Method development for correlated noise
  - Study the physical connection between signals due to different sources and the components recovered from PCA
  - Determine the feasibility of using PCA to reduce TEM data in UXO applications to the signal exclusively produced by UXO and UXO-like anomalies, and
  - Apply the developed algorithm to data examples and assess the effectiveness through discrimination/classification tests.
- Method development for inversion of processed data
  - Develop a method for parametric inversion of processed data for recovery of diagnostic parameters in UXO applications.

1.3 Project summary

In this report, we summarize the major research accomplishments of the SERDP MM-1640 project. In short, we have accomplished the main objectives of this project, leading to a workflow ready to be inserted into industry-standard practices for the improved detection of UXO in noisy environments.

In Chapter 2 we begin by presenting background material on principal component analysis which will be used throughout this report. We first develop necessary modifications to the basic PCA routines in Chapter 3 before presenting de-noising algorithms for both uncorrelated and correlated sources of noise. We continue in Chapter 3 by discussing requirements and procedures for large-scale PCA decompositions. We conclude the chapter by showing difficulties in inverting PCA-processed data and develop an algorithm for both parametric and non-parametric inversion of this processed data.

In Chapter 4, we provide a series of examples demonstrating the efficacy of PCA in transient electromagnetic survey processing. We begin by showing how PCA can remove uncorrelated noise in a field dataset from Kaho'olawe, HI. We then present a parametric inversion result showing that PCA can improve the recovery of diagnostic parameters for UXO/scrap metal discrimination. We conclude the examples by taking a dataset contaminated by correlated noise through a complete workflow in UXOLab both with and without processing by PCA. We show a marked reduction in the number of false anomalies without compromising the detection of actual UXO.

We conclude this report in Chapters 5 and 6 with a discussion of the project results, recommendations, and publications/presentations generated throughout the lifespan of SERDP Project MM-1640.

CHAPTER 2
BACKGROUND

2.1 Principal component analysis

Principal component analysis (PCA) is a statistical method for analyzing observations in multiple channels through an orthonormal projection. Not only does principal component analysis have the ability to separate and remove uncorrelated noise, but also to decompose a signal into constituent components from its sources in many cases. Consequently, PCA has been used for many different applications including digital image enhancement, facial recognition, data transmission and compression (Jones and Levy, 1987), de-noising radiometric data (Minty and Hovgaard, 2002), and seismic de-noising (Jones and Levy, 1987; Jackson et al., 1991), to name a few. Recently, PCA has been applied to airborne EM (AEM) surveys to construct intuitive RGB maps based on the principal components (Green, 1998). In other electromagnetic applications, Asten (2009) has used PCA in unexploded ordnance TEM surveys to classify targets, while Hu and Collins (2004), Hu et al. (2004), and Throckmorton et al. (2007) have used similar techniques using higher-order moments (Independent Component Analysis) to recover diagnostic parameters of differing ordnance items. The most common use of Principal Component Analysis in EM is to combine magnetic and electromagnetic datasets (e.g. Rose-Pehrsson et al., 1998).

Although PCA methods vary greatly in their application, all linear PCA algorithms are similar in that they deconstruct a multi-channel signal into a set of orthonormal bases of decreasing energy. These sets can be reconstructed into the original signal exactly, or a truncated set can be used in reconstruction that tends to eliminate noise. Correlated signals are typically reconstructed by added the bases (from highest to lowest energy) until the desired energy level is reached–generally chosen through a statistical analysis of error.

In most surveys with multiple stations that record traces (decay curves) of data, there are two organizations over which a signal can be said to be "correlated." One can analyze the correlation between time-slices or between traces. In essence, we are either analyzing similarities in anomaly geometry or similarities in decay. Which correlation we analyze will have important implications on computation cost of the calculations.

Geometrically, the data set from a TEM survey can be envisioned as a cloud of '$m \times n$' measurements in an n-dimensional data space (where m is the number of channels and n the number of stations, for purposes of this derivation). The data coordinate system is rotated until the first axis is along the direction where the data have the greatest variance. The second coordinate axis is chosen to have the next highest data variance subject to the constraint that it must be orthogonal to the first, and so on (Green, 1998). This is accomplished by using the eigenvectors of the covariance matrix as the new bases, as they will align with these directions of variance and will be mutually orthogonal.

To define these principal components, we introduce the Karhunen-Loéve Transform as a linear PCA tool as in Jones and Levy (1987). However, any eigenvector or singular value decomposition will produce an equivalent result to the accuracy of that decomposition (Minty and McFadden, 1998).

Assume a set of data consisting of multiple traces each with multiple data values

$$x_i(t_j),\ i = 1, ..., n;\ j = 1, ...m$$

where the i'th trace is associated with a particular location and the index j corresponds to a particular channel of observation at that given location. For example, one may have an EM63 instrument occupying n locations along a line or within a grid during a UXO survey, which would yield n traces of decaying voltage, each containing 25 channels of data ($m = 25$). As stated earlier, principal component analysis first generates a rotation matrix that rotates the data traces onto a set of orthogonal

directions called principal component directions. In such a rotation, the resulting components are ordered by decreasing energy. The earlier components with most energy tend to capture the coherent data signal whereas the later components tend to represent incoherent noise in the entire data set.

Such a rotation matrix can be defined by decomposing the covariance matrix $\mathbf{\Gamma}$ of the data traces. The elements of the covariance matrix are given by

$$\gamma_{kl} = \sum_{j=1}^{m} x_k(t_j)x_l(t_j), \quad k,l = 1,...,n. \tag{2.1}$$

The covariance matrix Γ can be decomposed into its corresponding eigenvalues and eigenvectors:

$$\mathbf{\Gamma} = \mathbf{R}\mathbf{\Lambda}\mathbf{R}^T, \tag{2.2}$$

where $\mathbf{\Lambda}$ is a diagonal matrix consisting of the eigenvalues of $\mathbf{\Gamma}$ and $\mathbf{R}$ is the eigenvector matrix whose columns are the corresponding eigenvectors. Kramer and Mathews (1956) showed that the eigenvectors define the principal component directions and matrix $\mathbf{R}^T$ is exactly a rotation matrix that decomposes (or rotates) the original signal into such components:

$$\psi_k(t) = \sum_{i=1}^{n} r_{ki}x_i(t) \quad k = 1,...,n, \tag{2.3}$$

and the original signal can be reconstructed by:

$$\tilde{x}_i(t) = \sum_{k=1}^{n} r_{ik}\psi_k(t), \quad i = 1,...,n. \tag{2.4}$$

Using a compact notation with a data matrix $\mathbf{X}$ whose rows are the data traces, the

decomposition ($\mathbf{\Psi}$) and reconstruction can be written as

$$\mathbf{\Psi} = \mathbf{R}^T\mathbf{X} \tag{2.5}$$

$$\tilde{\mathbf{X}} = \mathbf{R}\mathbf{\Psi}. \tag{2.6}$$

We note that the eigenvector matrix $\mathbf{R}$ is a unitary matrix and satisfies:

$$\mathbf{R}\mathbf{R}^T = \mathbf{R}^T\mathbf{R} = \mathbf{I},$$

where $\mathbf{I}$ is an identity matrix. Thus the reconstruction is exact and unique, and the data matrix $\mathbf{X}$ is equal to:

$$\mathbf{X} = \tilde{\mathbf{X}} = \mathbf{R}\mathbf{R}^T\mathbf{X}. \tag{2.7}$$

Mathematically, the reconstructed signal is exactly equal to the original signal when all principal components are included. Reconstructing with a selected subset of principal components $\psi_k(t)$ would yield a truncated reconstruction that is devoid of the energy captured in the discarded components. For example, incoherent noise often populates the last few principal components and discarding them during reconstruction would yield a cleaner signal that is minimally affected by the noise. Thus to perform simple de-noising of signals, the reconstruction series is truncated as:

$$\tilde{x}_i(t) = \sum_{k=1}^{c} r_{ik}\psi_k(t) \quad c \leq n, \tag{2.8}$$

although other reconstruction schemes are also possible. In matrix notation:

$$\begin{aligned} \tilde{\mathbf{X}} &= \mathbf{R}\mathbf{B}\mathbf{R}^T\mathbf{X} \\ \tilde{\mathbf{X}} &= \mathbf{Y}\mathbf{X}, \end{aligned} \tag{2.9}$$

where $\mathbf{B}$ is a diagonal matrix, with ones at the rows corresponding to the components

used for reconstruction, and zeros everywhere else. This result is derived from the fact that PCA measures *correlated* energy. If a signal is random from trace to trace then there is very little correlated energy between the signals, so the reconstruction of those signals falls to the later components. For this reason, truncation of the rotated matrix is an extremely fast process to remove uncorrelated noise from the data.

CHAPTER 3

ALGORITHM DEVELOPMENT

3.1 Introduction

The PCA algorithm for UXO surveys follows the same general pattern as described in Chapter 2. However, significant changes need to be made depending on whether temporal or spatial correlation of the data is chosen. Temporal correlation requires significant data regularization before calculation of the covariance matrix, while spatial correlation may require a distance function applied to the correlation. In addition, with spatial correlation the covariance matrix can become extremely large, precluding a complete eigenvector decomposition. Thus more efficient eigenvector decomposition techniques are required.

Once decomposition into principal components is complete, proper choice of which principal components used in reconstruction is critical. This choice is dependent on the types of signal that need to be attenuated. Since the orthogonal bases are data-dependent instead of user-chosen, the principal components used in reconstruction are entirely a function of the signal to be removed, and are common throughout all types of surveys.

The reconstructed data no longer has the same decay characteristics as before, so the same inversion kernels can not be used to invert PCA-processed data. We therefore developed an inversion algorithm for both parametric and generalized inverse cases.

This chapter describes the algorithm we developed, from data normalization to inversion. In general, PCA follows the workflow as described in figure 3.1.

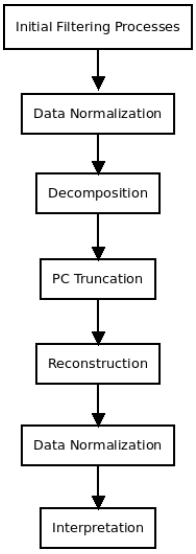

Figure 3.1. General workflow for processing TEM data with principal component analysis

3.2 Principal component analysis for transient electromagnetic surveys

In order to appropriately apply principal component analysis to TEM surveys, we must first define how we correlate our data. We may either correlate TEM data in terms of space or in terms of time. Spatial correlation relates variances between decay curves, while temporal correlation relates variances in time-intersects. For time domain surveys, construction of the covariance matrix must be modified from the standard definition as described in equation 2.1. The subsequent processing steps described earlier may be directly applied to this normalized data.

3.2.1 Temporal correlation

Temporal correlation relates variances in time-intersects. This method of organization is extremely useful for separating signals which have different decay characteristics, such as UXO and magnetic soils.

While most multi-channel data can be decomposed using the simple covariance matrix formulation shown in equation 2.1, the particular characteristics of TEM data

sorted by time preclude this construction. Since the signal decays exponentially with time, the data change in magnitude over several orders with a non-linear corresponding change in error level. This results in a poorly scaled covariance matrix, which results in inaccurate eigenvector decomposition. Most of the covariance is contained in the first few time gates, overwhelming the later gates. In addition, for certain surveys where magnetic soil is present such as at Kaho'olawe, a large signal (t^{-1} decay) dominates the data. Figure 3.2 shows an example covariance matrix for an EM-63 survey before and after the scaling is applied. This scaling is critical for accurate processing.

In order to properly scale the covariance matrix, we apply normalization to the data before processing. Let $\mathbf{X}$ be defined as a data matrix with an individual row corresponding to an individual decay curve or trace.

Let $\mathbf{b}$ be defined as

$$\mathbf{b}_j = \mathbf{x}_j - \frac{(\sum_{i=1}^{n} x_{ij})}{m} \tag{3.1}$$

where m is the number of time gates, $\mathbf{x}_j$ is a row vector containing an individual trace, and n is the number of observation locations. We then define the standard deviation for the j^{th} time gate as

$$\sigma_j = \left(\sum_{i=1}^{n} b_{ij}^2 \right)^{1/2}. \tag{3.2}$$

We then normalize the data by the first time gate of each curve as

$$\mathbf{x}_i \leftarrow \frac{\mathbf{x}_i}{x_{i,1}}. \tag{3.3}$$

(Please note we use an assignment statement rather than an equality simply because we have run out of letters.) The final step is to normalize the data by the standard

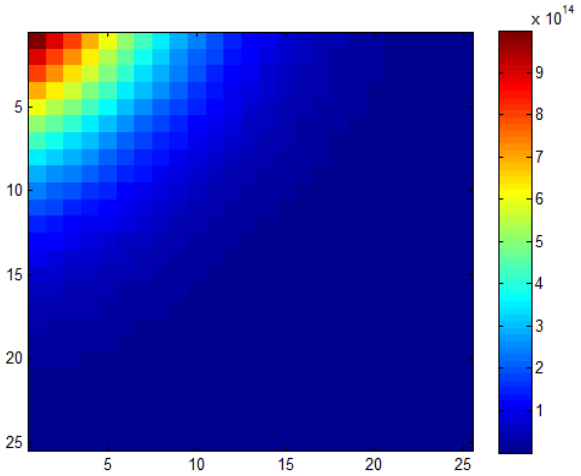

(a)

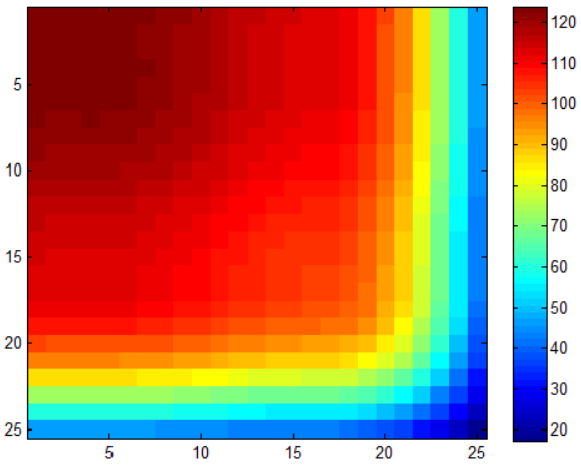

(b)

Figure 3.2. Covariance calculations (a) before and (b) after normalization of the data.

deviations calculated in equation 3.2:

$$\mathbf{x}_j \leftarrow \frac{\mathbf{x}_j}{\sigma_j}. \tag{3.4}$$

The correlation matrix is then calculated from this normalized data. As described in detail in Chapter 2, the data undergo an orthogonal transformation to a basis spanned by the eigenvectors of this new covariance matrix. Principal components are chosen to be removed (the choice of which are described in sections 3.3 and 3.4), and the data are rotated back, leaving a dataset with unwanted features removed or attenuated. It is important to note that at the end of PCA processing, the data must be un-normalized by applying the above procedure in reverse order to the processed data.

3.3 Removal of uncorrelated noise

The removal of uncorrelated noise generally involves the removal of the last few principal components–those corresponding to the smallest eigenvalues. The choice of how many principal components to remove can be made by following a general guideline based on the estimated noise threshold. The principal components are removed until the sum of their associated eigenvalues relative to the total is equal to the estimated noise level. For example, if we estimate 5% random noise in our survey data, then we remove principal components starting with the last one until the sum of the associated eigenvalues divided by the total sum of the eigenvalues equals 0.05.

These principal components are removed by applying a truncation matrix to the rotated data, as described in equation 2.9. The truncation matrix starts as an identity matrix, where elements on the diagonal are replaced with zeros corresponding to the principal components to be removed.

3.4 Removal of correlated noise

The process of removal of correlated noise is dependent on the type of noise to be removed. This type of noise can be classified into two types, each having a distinct and well-defined method for removal: static and variable.

Static noise includes sources such as magnetic soils, which exhibit decay proportional to t^{-1}, and sensor orientation, which behaves like a static shift for small perturbations of the orientation of receiver/transmitter coils. These sources of noise tend to effect large areas of the survey grid and have a temporally-invariant signature. These noise sources map into the first principal component, thus removal of the first principal component will attenuate these signals. Removal of the first principal component will also remove a portion of the signal due to UXO, but will leave the diagnostic decay characteristics intact (Figures 4.8 and 4.10). Section 3.8 describes how to interpret the data after processing while incorporating this effect.

Variable noise includes signals from telluric currents, RF interference, and similar signals. These are more temporally and spatially variable, and will thus map into principal components smaller than those containing the UXO. Therefore, in surveys where noise sources such as these are known to be present, only the first two principal components can generally reconstruct the signal due to UXO, while the signal due to this noise is attenuated.

3.5 Spatial correlation

Spatial covariances relate changes in anomaly geometry across a survey rather than changes in decay characteristics. While this method of organization is less useful for UXO applications than temporal correlation, the method can still be useful in applications for removal of large geologic features.

Initial construction of the covariance matrix requires no special normalization of the data as the variation in measured magnitude across a single time-intersect is much smaller than across a decay curve. However, choice of principal components to

remove is no longer clear and requires significant user input. How a particular UXO item maps into the principal component space is highly dependent on the spatial characteristics of the geology–much more so than in a temporal correlation. Thus trial and experience are critical for proper choice of principal components for reconstruction. As a consequence of this dependence, UXO can map into a much wider variety of principal components. Therefore calculating the first few eigenvectors to save computation time is not an appropriate approach to the problem. Since the covariance matrix in this construction has n^2 elements, where n is the number of data traces, the matrices can be extremely large.

For these reasons, we do not recommend the use of spatially-correlated covariances as a component of a standard UXO workflow. However, cases may exist where strong spatially-variant features have the same decay characteristics as UXO, and the spatial correlation must be taken advantage of. Section 3.6 discusses numerical techniques to address these issues.

3.6 Large-scale decompositions

When correlating data spatially, the covariance matrices can become extremely large. Thus efficient methods of eigenvector decomposition must be used. Two basic approaches can be taken: decimating the covariance matrix to make it sparse, or utilizing efficient eigenvector decomposition algorithms.

Decimating the covariance matrix involves assuming that certain data locations must have zero correlation, usually due to distance. Applying a distance weighting function to the covariance calculation, whether smooth or binary, can result in a sparse matrix. As an example of a smooth weighting function, we apply a distance weight to the covariance calculation:

$$\gamma_{kl} = \sum_{j=1}^{m} x_{kj} x_{lj} \left(1 - \frac{\alpha \sqrt{(y_k - y_l)^2 + (z_k - z_l)^2}}{\sqrt{\max(y_i - y_0)^2 + \max(z_i - z_0)^2}} \right), \quad i, k, l = 1, ..., n \qquad (3.5)$$

where y, z are Cartesian coordinates of each data location, and α is some constant that controls the radius of inclusion. By choosing an appropriate algorithm that utilizes this sparsity, the computation time and memory requirements can be greatly reduced.

Because of the size and potentially sparse nature of the spatial covariance matrices, iterative methods for eigenvector decompositions are most appropriate for PCA. There are many to choose from, each with advantages and disadvantages, and no one decomposition is perfect in all cases. However, we briefly review the most applicable iterative methods to UXO here. For further details on each of these algorithms, we refer the reader to Blackford (2000).

3.6.1 Iterative eigenvalue decompositions

Lanczos method

The Lanczos method is one of the most widely used algorithms for large-scale eigenvector decomposition. By building up Ritz approximations to the eigenvalues of the matrix, the Lanczos method produces several eigenvalues from once sequence of vectors that converge quickly. Unfortunately, even mildly ill-conditioned matrices produce a system which destroys orthogonality quickly, requiring a reorthogonalization process (i.e. Gram-Schmidt).

Power method

The power method is the most simple of the methods to implement. However, the process, like many of the other methods, begins at one extreme eigenvalue and calculates each subsequent eigenvalue–finding a subset of interior eigenvalues requires a shift-and-invert modification.

Subspace iteration method

This method is extremely common in engineering applications, and may be the most readily applied process to PCA due to its prevalence in the community. Much like the power method, however, the subspace iteration method directly produces only leading eigenvalues and eigenvectors.

Jacobi-Davidson method

The Jacobi-Davidson method can directly produce a cluster of interior eigenvalues without calculating the entire set by using preconditioners, making it extremely useful in spatially-correlated matrices.

3.7 Anomaly selection

Once PCA has been performed on a dataset, the data are ready for processing with automated anomaly picking routines such as with UXOLab, or manual interpretation. Each of the chosen anomalies can then be further processed with numerical inversion techniques or other discrimination algorithms.

3.8 Inversion of processed data

While inversion of electromagnetic data is a nonlinear process, insight into the requirements for inversion of PCA-processed data can be gleaned from studying a linear as well as nonlinear case. Linear inversion of geophysical data seeks to invert the forward mapping operator (or sensitivity matrix), $\mathbf{G}$ that operates on the model to produce measured data. This inverted matrix may then be applied to the data to map them back into the model space. In general, noise must be accounted for and the problem is ill-posed. Thus further information, such as constraints on the size or structure of the model, reference models, data weighting, and many others is required for a stable inversion (Oldenburg and Li, 2005). Allowing a trade off between

the model norm (ϕ_m) and the data misfit (ϕ_d), leads to the global objective function which is minimised to arrive at the Tikhonov solution:

$$\phi = \phi_d + \beta\phi_m. \tag{3.6}$$

Inverting for the smallest model with an L_2 data misfit measure, the minimization of this solution expands to:

$$(\mathbf{G}^T\mathbf{G} + \beta\mathbf{I})\mathbf{m} = \mathbf{G}^T\mathbf{d} \tag{3.7}$$

and $\mathbf{m}$ can be solved for either directly or iteratively using the conjugate gradient or similar solution. The Tikhonov or regularization parameter, β, is either chosen such that an optimal data misfit is reached, by using the L-curve criterion (Hansen, 1992), or a generalized cross validation (GCV) approach.

The forward mapping operator described here encompasses the physics and geometry of the geophysical problem. Once data has been processed with PCA for signal isolation or de-noising, this forward mapping operator no longer accurately maps the model to this new rotated data as the data have been rotated to a new basis in $\mathbb{R}^n$. In order to accomplish this mapping (and thus inversion), the forward mapping operator must also be rotated such that it maps from the model space to this new data space.

We apply the rotation matrix to each column of the sensitivity matrix, $\mathbf{G}$, individually to match the processed data, $\mathbf{d}_{rot}$. This is equivalent to multiplying a new matrix $\mathbf{Y}_g$ to the sensitivity matrix, where $\mathbf{Y}_g$ is a block-sparse matrix with the original rotation matrix $\mathbf{Y}$ on the diagonal as:

$$\mathbf{Y}_g = \begin{bmatrix} \mathbf{Y} & 0 & \dots & 0 \\ 0 & \mathbf{Y} & & \\ \vdots & & \ddots & \vdots \\ 0 & & \dots & \mathbf{Y} \end{bmatrix} \tag{3.8}$$

Thus Equation 3.7 becomes

$$((\mathbf{Y}_g\mathbf{G})^T(\mathbf{Y}_g\mathbf{G}) + \beta\mathbf{I})\mathbf{m} = (\mathbf{Y}_g\mathbf{G})^T\mathbf{d}_{rot} \tag{3.9}$$

and can be solved with the same numerical methods as before. It is important to note that $\mathbf{Y}$ and $\mathbf{Y}_g$ are both positive-semidefinite since they are calculated from the eigenvectors of the covariance matrix.

The general solution to a non-linear inverse problem is solved by developing a locally linear system and minimising the objective function described in Equation 3.6. We then update our sensitivity matrix and continue in an iterative process until the global objective function is minimised via a Gauss-Newton or similar method. In the case where no rotation on the data has been performed, we may develop our global objective function with a data misfit and model norm to be minimised which expands to:

$$\phi(\mathbf{m}) = \|\mathbf{W}_d(\mathbf{d}_{obs} - F[\mathbf{m}])\|^2 + \beta\|\mathbf{W}_m(\mathbf{m} - \mathbf{m}_{ref})\|^2 \tag{3.10}$$

where $\mathbf{m}$ is the vector of parameters, $\mathbf{d}_{obs}$ is the recorded data with a corresponding weighting matrix $\mathbf{W}_d$, F is the forward mapping operator (that depends on $\mathbf{m}$), β is a Tikhonov or regularization parameter, $\mathbf{m}_{ref}$ is a reference model, and $\mathbf{W}_m$ a corresponding weighting matrix.

In general, the local linear system can be obtained through a perturbation approach using the Gauss-Newton method with the following form:

$$\begin{aligned}\left(\mathbf{J}^T\mathbf{W}_d^T\mathbf{W}_d\mathbf{J} + \beta\mathbf{W}_m^T\mathbf{W}_m\right)\delta\mathbf{m} = \\ \mathbf{J}^T\mathbf{W}_d^T\mathbf{W}_d\left(\mathbf{d}_{obs} - F\left[\mathbf{m}^{(n)}\right]\right) - \beta\mathbf{W}_m^T\mathbf{W}_m\left(\mathbf{m}^{(n)} - \mathbf{m}_{ref}\right)\end{aligned} \tag{3.11}$$

where $\mathbf{J}$ is a Jacobian matrix. In order to generalize the forward mapping such that the rotation and possible truncation of the data is included, we apply the same rotation operator to the data predicted by the forward operator F, just as in the linear case. This leads to an altered equation 3.11:

$$\left(\mathbf{J}_{rot}^T\mathbf{W}_d^T\mathbf{W}_d\mathbf{J}_{rot} + \beta\mathbf{W}_m^T\mathbf{W}_m\right)\delta\mathbf{m} =$$
$$\mathbf{J}_{rot}^T\mathbf{W}_d^T\mathbf{W}_d\left(\mathbf{d}_{rot} - \mathbf{Y}_g F\left[\mathbf{m}^{(n)}\right]\right) - \beta\mathbf{W}_m^T\mathbf{W}_m\left(\mathbf{m}^{(n)} - \mathbf{m}_{ref}\right) \tag{3.12}$$

where $\mathbf{d}_{rot}$ is the rotated data and $\mathbf{Y}_g$ is the same matrix defined in Equation 3.8. The inversion can be computed in the same way as before. Since the Jacobian matrix is calculated from the predicted data, the rotation matrix will be combined into the Jacobian, $\mathbf{J}_{rot}$, with each subsequent step, so explicit rotation of the Jacobian is unnecessary.

Alteration of the original data by a transform also modifies the statistical distribution of the noise. After PCA, ideally there is no random noise and all signal is a result of coherent sources (whether geologic or otherwise). This would imply that in an ideal separation case, the Tikhonov parameter β would approach zero to maximally weight a data misfit of zero. Clearly this case is not achieved for several reasons: data errors are not always zero bias with a Gaussian distribution (or any other uncorrelated distribution), PCA has intrinsic numerical error in the calculation of eigenvectors, there is strongly correlated noise associated with most surveys, and original statistical estimates for error removal may have been incorrect in the first place (i.e. which principal components to use). Therefore the data misfit is guaranteed to not have a χ^2 distribution. So while the value of the data misfit is defined, the appropriate value of data misfit for an optimal solution is not. However, this altered data misfit can be treated while choosing β with the L-curve criterion or with a generalized cross validation approach–both work regardless of the rotation applied.

The same approach to inverting rotated data in a generalized inversion applies equally to a parametric inversion. In the parametric case, the global objective function does not contain a model objective (as the model is defined explicitly already), and

1	Perform any initial filtering (such as median filtering), if necessary
2	Normalize data (3.2.1)
3	Data decomposition (2.1)
4	Principal component truncation (2.1, 3.3, and 3.4)
5	Reconstruction (2.1)
6	Remove data normalization (3.2.1)
7	Application of anomaly automatic picking routines, such as in UXOLab (3.7)
8	Numerical inversion of individual anomalies (3.8)

Table 3.1. Recommended PCA algorithm. Numbers in parentheses correspond to sections with detailed descriptions.

so a Gauss-Newton solution to a parametric case with rotated data becomes

$$\left(\mathbf{J}^T\mathbf{W}_d^T\mathbf{W}_d\mathbf{J}\right)\delta\mathbf{m} = \mathbf{J}^T\mathbf{W}_d^T\mathbf{W}_d\left(\mathbf{d}_{obs} - \mathbf{Y}_g F\left[\mathbf{m}^{(n)}\right]\right).$$

As in the full generalized inversion, the rotation matrix should not be explicitly applied to the Jacobian.

3.9 Algorithm summary

In this chapter we have introduced a PCA algorithm for processing TEM data to attenuate both uncorrelated and correlated noise, as well as developed an inversion algorithm for interpretation of individual UXO anomalies. Table 3.1 shows a skeleton algorithm for the processing and interpretation of TEM data with PCA. In the next chapter, we show examples of the successful application of PCA to TEM data.

CHAPTER 4
RESULTS

In this chapter we present three examples of the successful application of PCA to unexploded ordnance detection and discrimination. These examples show the varied applications and contributions of PCA to detection and discrimination of UXO, as well as the ease of insertion into a standard workflow.

4.1 Uncorrelated noise removal

To show the de-noising capability of PCA, we present an example dataset from Kaho'olawe, Hawaii, USA. The TEM data (collected with a Geonics EM63) come from a 30 metre by 60 metre grid set on extremely magnetic soils (magnetite, titanomagnetite, and ilmenite) due to volcanism. Weathering of the volcanics in the tropical climate led to soils exhibiting a high degree of frequency dependence in magnetic susceptibility. The spatially variable, frequency-dependent susceptibility produces strong $1/t$ decay that masks the UXO response in EM63 data. The soil response is over 400 mV in the first gate across the survey area (Figure 4.1). In addition, the instrument movement, ambient interferences, and other sources lead to the ubiquitous noise in late time gates.

To assist with the separation of the magnetic soil response from unexploded ordnance, we must first attenuate the noise in the late time gates. The strong soil response masks much of the signal due to UXO before the last few time gates, so improvement in signal-to-noise is paramount in interpretation.

The data (consisting of 23000 decay curves of 25 gates each) were decomposed into constituent principal components and re-composed using a subset of those components. Figure 4.2(a) shows a set of the original data that include only geologic response as well as data that have signal from UXO imprinted on the decay curves.

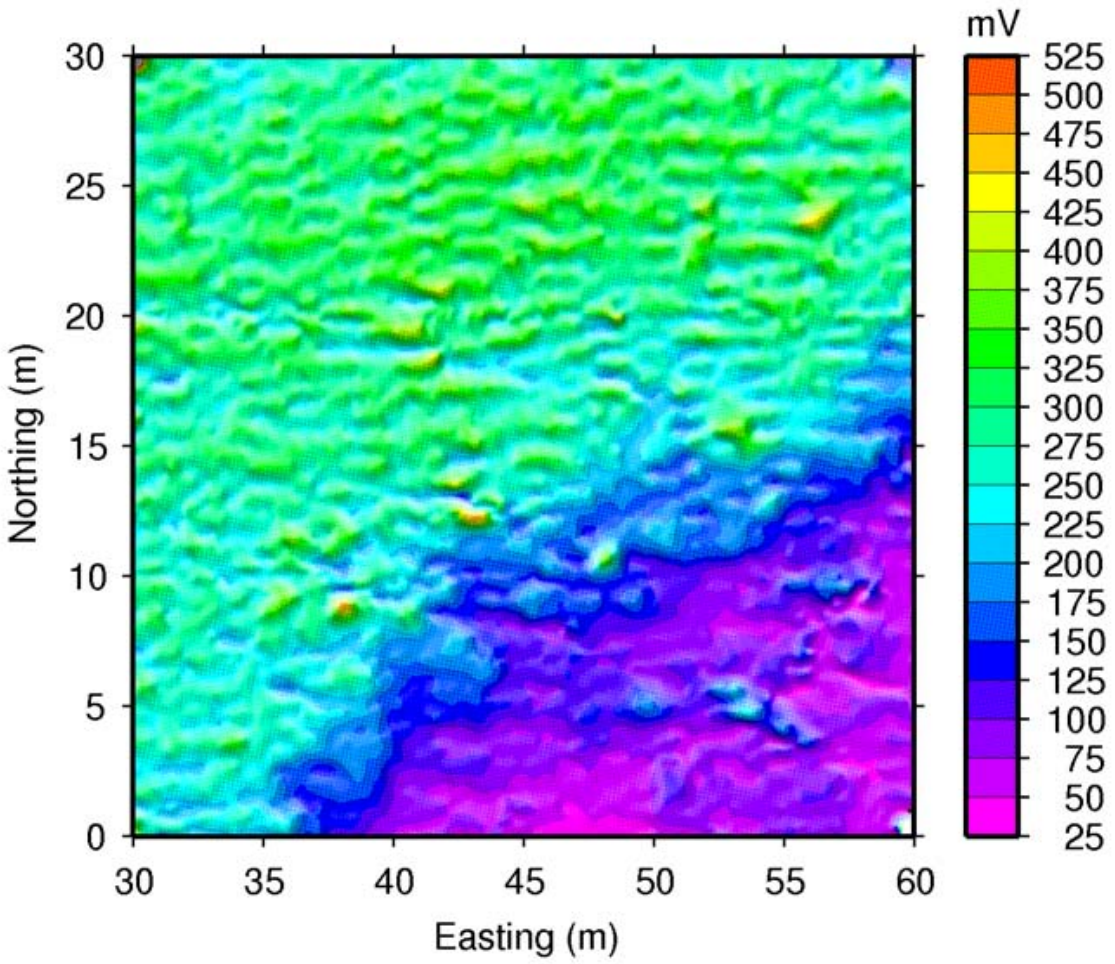

Figure 4.1. First time gate of EM63 data collected over the Kaho'olawe Navy QA grid. Note the large geologic response due to viscous remnant magnetization (VRM).

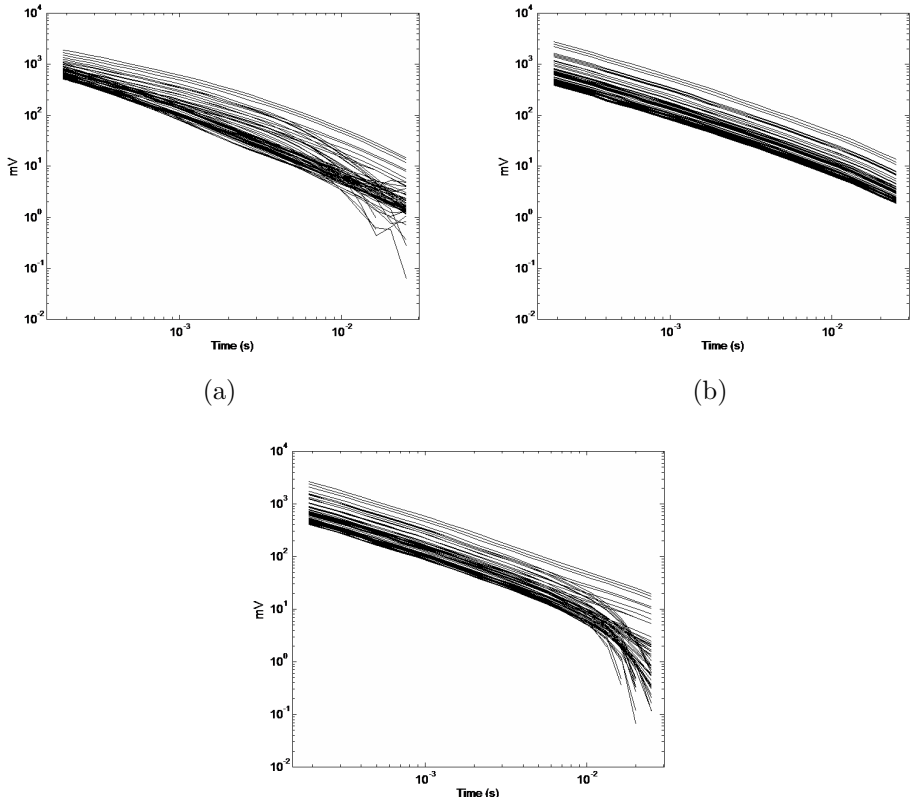

Figure 4.2. (a) 65 example decay curves from Kaho'olawe. Some traces include responses from unexploded ordnance; these traces deviate from the expected t^{-1} decay. (b) Geologic response constructed with only the first principal component. The curve exhibits the expected inverse power law decay due to horizontal layering and magnetic soils. (c) TEM decay curves constructed with the first and second principal components. The (approximate) superposition of UXO signal on the geologic signal is clear, with significant reduction of random noise in later channels. (Negative values not displayed)

Magnetic soil at Kaho'olawe (and in general) exhibits a t^{-1} decay in TEM surveys (Pasion et al., 2002). This signal is clearly present in the raw data (Figure 4.2(a)). Reconstruction with only the first principal component reveals this decay due to the magnetic soil (Figure 4.2(b)). Traces with UXO and those without UXO are indistinguishable. However, when the second principal component is added (Figure 4.2(c)), the signal from the UXO (deviation from t^{-1} decay in later time gates) is clear. The random, uncorrelated noise that contaminated these later time gates is severely reduced without attacking the amplitudes of the decay curves, preparing them for numerical discrimination analysis with other methods.

4.2 Inversion of processed data

4.2.1 Linear inversion

As an example of the need to include the rotation matrix in inversion, we present the following linear example. The model, m, consisting of one-thousand elements, is represented by a sine function of the form

$$m(x) = 1 - .5[\cos(2\pi x) + \sin(2\pi x)]$$

with 10 channels of data calculated at each of 11 data locations simulated (110 total data). The channels all utilize exponentials as kernels with different decay parameters and are functions of current and adjacent observation locations with 5% Gaussian noise. Thus we have a linear, underdetermined system to invert for the model parameters.

For the first case where no principal component analysis was applied, we inverted the data for the smallest model. The Tikhonov parameter, β, was chosen through the L-curve criterion. Because our chosen kernels are sensitive to noise, the smallest-model solution yields a poor recovered model (Figure 4.3(a)). Even though the optimal data misfit is reached, the structure of the recovered model is poorly con-

strained at depth. The imprinted noise on the underdetermined problem is preventing a good result, despite an excellent L-curve (Figure 4.4(a)).

As a de-noising tool, principal component analysis is a logical choice to reduce the uncorrelated noise present in the data. Therefore, we applied a blind PCA to the data, where the amount of energy contained in the noise was estimated and latter principal components were removed to reach 5% noise, nulling all but the first two principal components. The data were then rotated back and inverted again with the same sensitivity matrix as before to yield the model in Figure 4.3(b). Though the shallow structure has improved, it still does not accurately represent the true model. In addition, choice of regularization parameter was more ambiguous than the previous case, as the L-curve contained two areas of high curvature (Figure 4.4(b)).

To improve the recovered model, we applied the rotation matrix to the sensitivity matrix as described in this paper. With the sensitivity matrix consistent with the data space, the inversion produced a much better result (Figure 4.3(c)). Moreover, the optimal β term was easy to choose from the L-curve (Figure 4.4(c)).

4.2.2 Non-linear inversion

We present synthetic data from an unexploded ordnance survey. We simulate data from a 25 channel transient electromagnetic survey (such as with a Geonics EM-63, for example) over a half-space with a 75mm mortar round buried at 1 m depth. We use the Pasion-Oldenburg parametric model that uses two dipolar responses to simulate the signal from the mortar round. Each dipole decays as:

$$k(t+\alpha)^{-\beta}e^{-t/\gamma} \tag{4.1}$$

where the parameters k, α, β, and γ depend on the conductivity, permeability, size, and shape of the object. The ratios of certain values can then be used as diagnostic indicators for unexploded ordnance (UXO) candidates.

We parametrically invert the synthetic dataset for the UXO parameters with

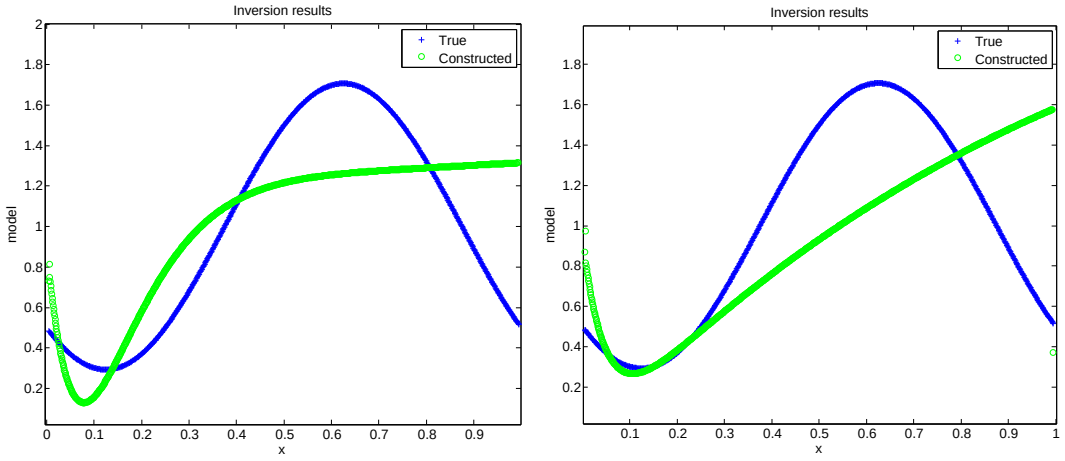

(a)

(b)

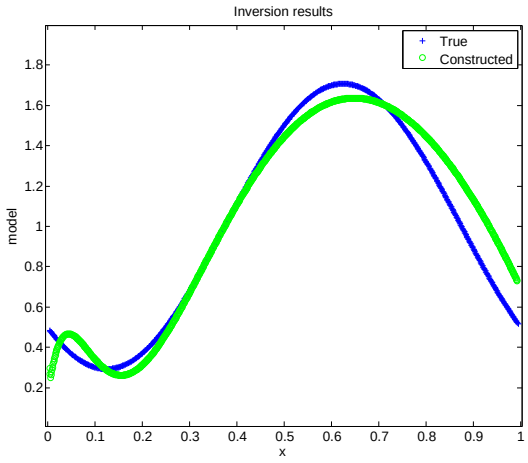

(c)

Figure 4.3. Original and recovered model (a) through smallest model solution, (b) after PCA on data only, and (c) after PCA on data and kernels.

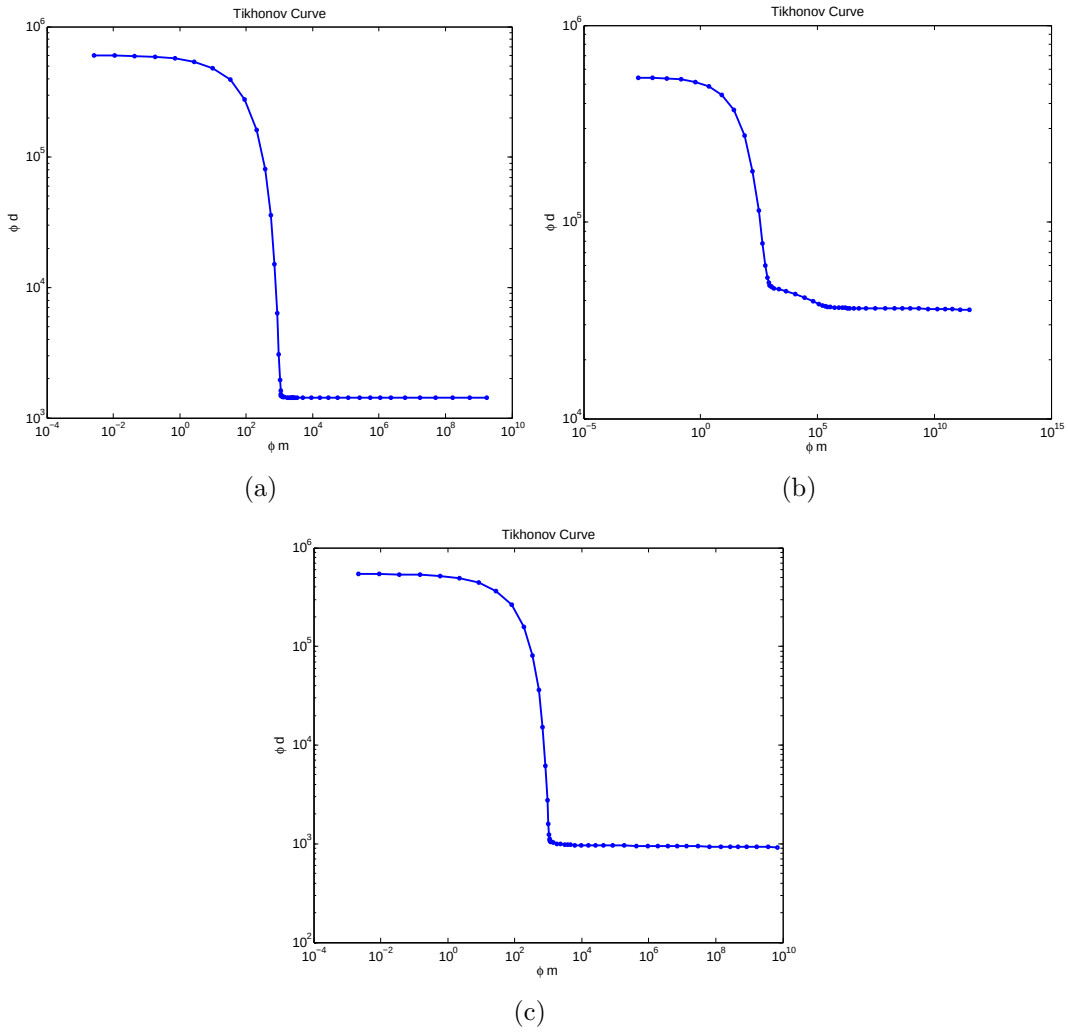

Figure 4.4. L-curve for (a) original inversion, (b) inversion with rotated data, and (c) inversion with rotated data and rotated sensitivity matrix.

	Original Inversion		PCA-Processed		PCA Incorporated	
	Recovered	Diagnostic	Recovered	Diagnostic	Recovered	Diagnostic
k1/k2	0.65	x	0.65	x	10.9	√
β1/β2	0.96	√	1.02	x	0.9	√
β avg	0.92	√	0.92	√	1.04	√

Table 4.1. Nonlinear inversion results. Only by applying PCA to both the data and the kernels were we able to properly recover diagnostic parameters.

the intention of recovering the proper diagnostic ratios. The objective function is constructed in the same manner as before, save that there is no model weighting (since this is a parametric inversion). Thus the linearized system to solve becomes:

$$\left(\mathbf{J}^T\mathbf{W}_d^T\mathbf{W}_d\mathbf{J}\right)\delta\mathbf{m} = \mathbf{J}^T\mathbf{W}_d^T\mathbf{W}_d(\mathbf{d}_{obs} - F\left[\mathbf{m}^{(n)}\right]). \tag{4.2}$$

We solve this system for noisy data, PCA-processed data, and PCA-processed data with the rotation matrix incorporated into the inversion. Table 1 shows the results. Inverting the data with no processing fails to recover the k ratio, which contains shape information. Processing the data with PCA but not incorporating the rotation matrix into the inversion results in incorrect recovery of all shape information. Only by incorporating the rotation matrix do we successfully identify a potential UXO target.

4.3 Correlated noise removal

Variations in the orientation of the TEM transmitter and receiver cart due to microtopography can produce significant signal in the data. Figure 4.5 shows the first time gate recorded in a synthetic EM-63 survey. This survey used real orientation vectors from a UXO survey and simulated the TEM response of the orientation errors and 40 mm mortar shells. Large, linear trends can be seen in the data where an approximate static shift in amplitude across all time gates has been introduced.

This type of correlated noise often has a large effect on autopicking routines.

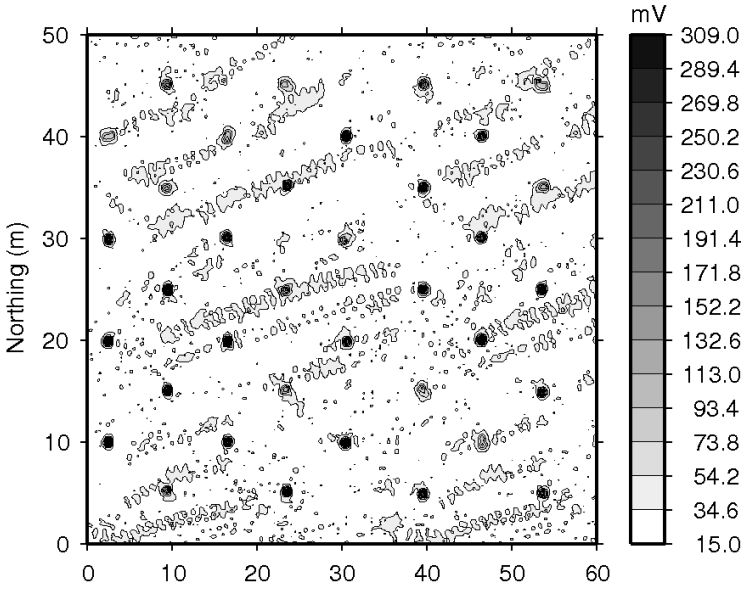

Figure 4.5. Effect of cart orientation error in a UXO survey. Orientation error produces an approximate 50 mV response in this example, visible in the approximate east/west lineations.

The characteristics of correlated noise sources are often similar enough to those of UXO that autopicking routines cannot differentiate them. Moreover, the frequency contents of the signals overlap such that frequency filtering is difficult or impossible. Figure 4.6 shows the radially-averaged power spectra of the constituent components in the dataset shown in Figure 4.5. The power spectra of signal due to cart orientation error concentrates power in the same bands as the signal due to UXO. Therefore separation using simple frequency filtering is impossible (Figure 4.7). Processing the dataset in Figure 4.5 with UXOLab's (UXOLab, 2009) autopicking routines leads to 60 targets (after clustering the picks). Figure 4.8 shows the picked anomalies using the routines provided in UXOLab. The effect of the cart orientation on the picking routine is clear–large numbers of false positives result.

Effects due to cart motion effectively result in an approximate static shift in the data. Therefore the orientation error effects each time gate equally. Thus to remove this effect, the first principal component was removed. Figure 4.10 shows the dataset

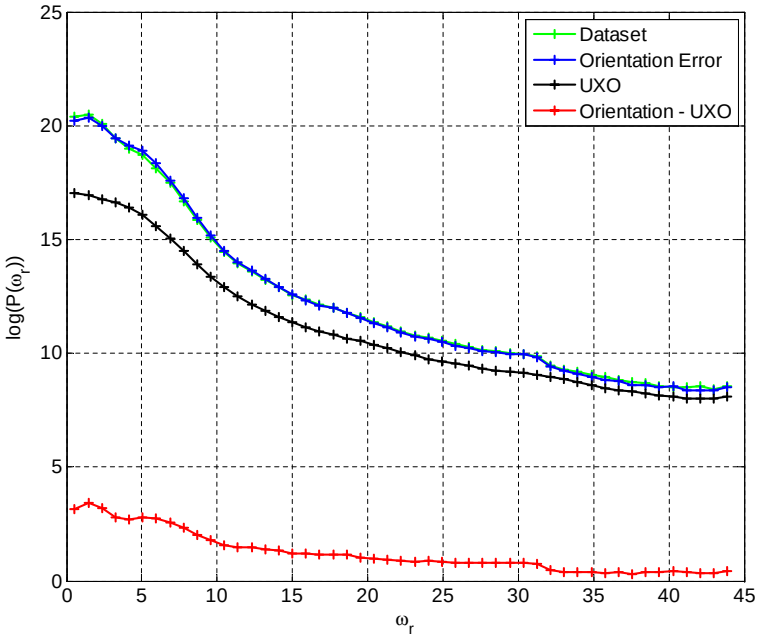

Figure 4.6. Radially averaged power spectrum of the original data set, orientation error, and UXO signal. The difference between the power spectra of the orientation error and the UXO signal indicates that they are inseparable in the frequency domain.

with the cart orientation error removed. Though the amplitude of the UXO anomalies have been reduced, the shape has been preserved.

This dataset was then processed in UXOLab for automatic UXO anomaly picking. Figure 4.9 shows two example lines from one time gate in this dataset. Figure 4.9(a) shows a line that passes through signals due to both UXO and cart orientation error. For autopicking purposes, a threshold of 50 mV was chosen based on the signals present in this line. This resulted in the picks previously shown in Figure 4.8. After principal component analysis, a threshold of 8 mV was chosen (Figure 4.9(b)). Though visually this line does not appear to be improved, the new threshold dramatically improved the autopicking ability. Figures 4.9(c) and 4.9(d) show a line that does not pass through a UXO target, but does pass through signal due to cart orientation error. The signal due to orientation error is completely eliminated.

While the original dataset had 62 picks after clustering (Figure 4.8), the pro-

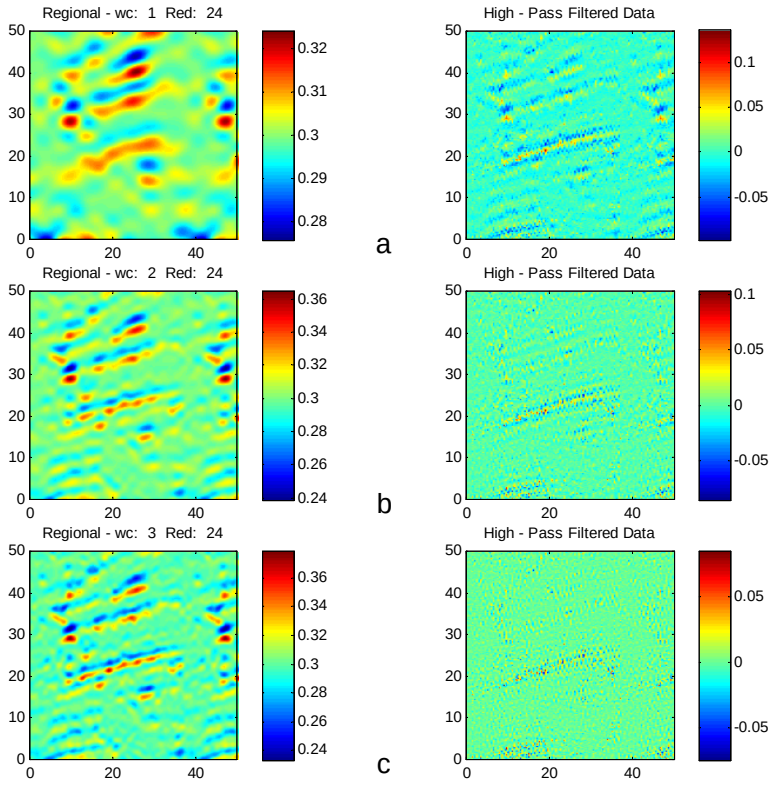

Figure 4.7. Three different examples of Butterworth filtering. The filtering is unable to separate the cart orientation error and UXO for a variety of cutoff wavenumbers.

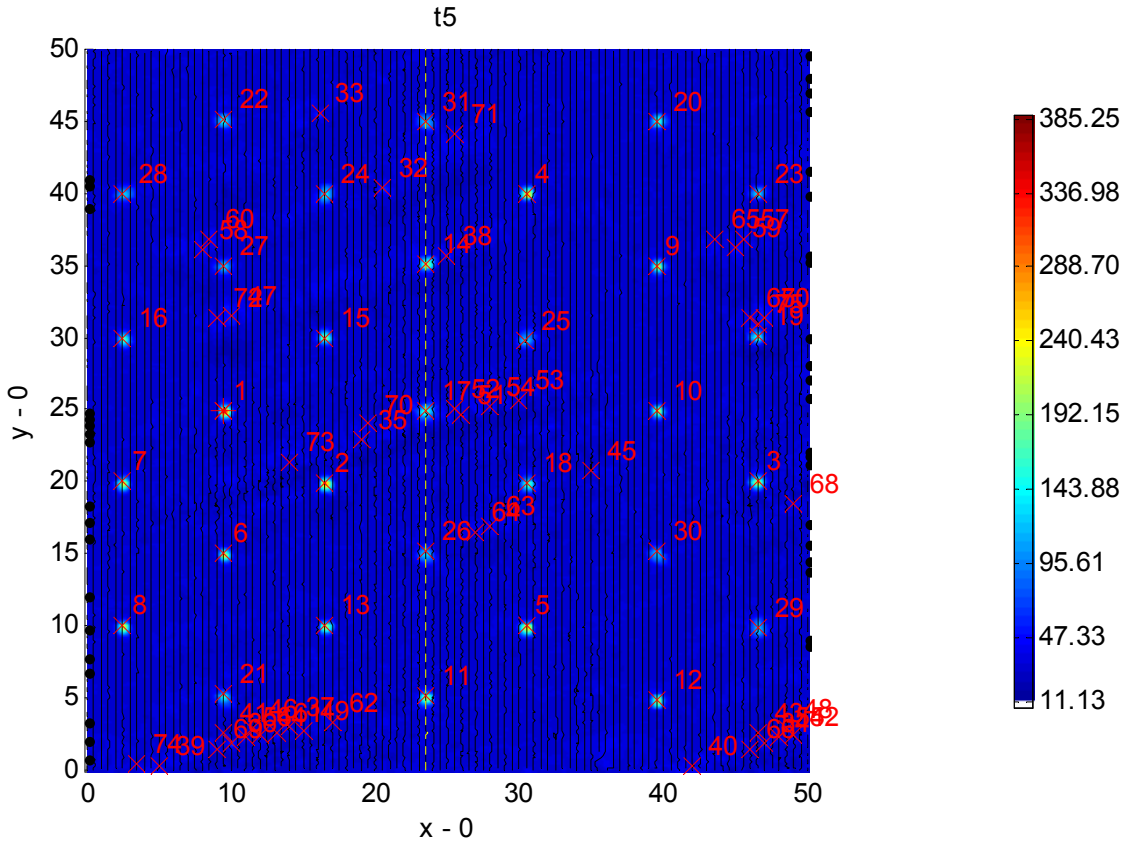

Figure 4.8. UXOLab target picks in a dataset contaminated with orientation error. Note the large number of picks corresponding to the cart orientation error (linear bands of picks). The dashed line corresponds to transects shown in Figure 4.9.

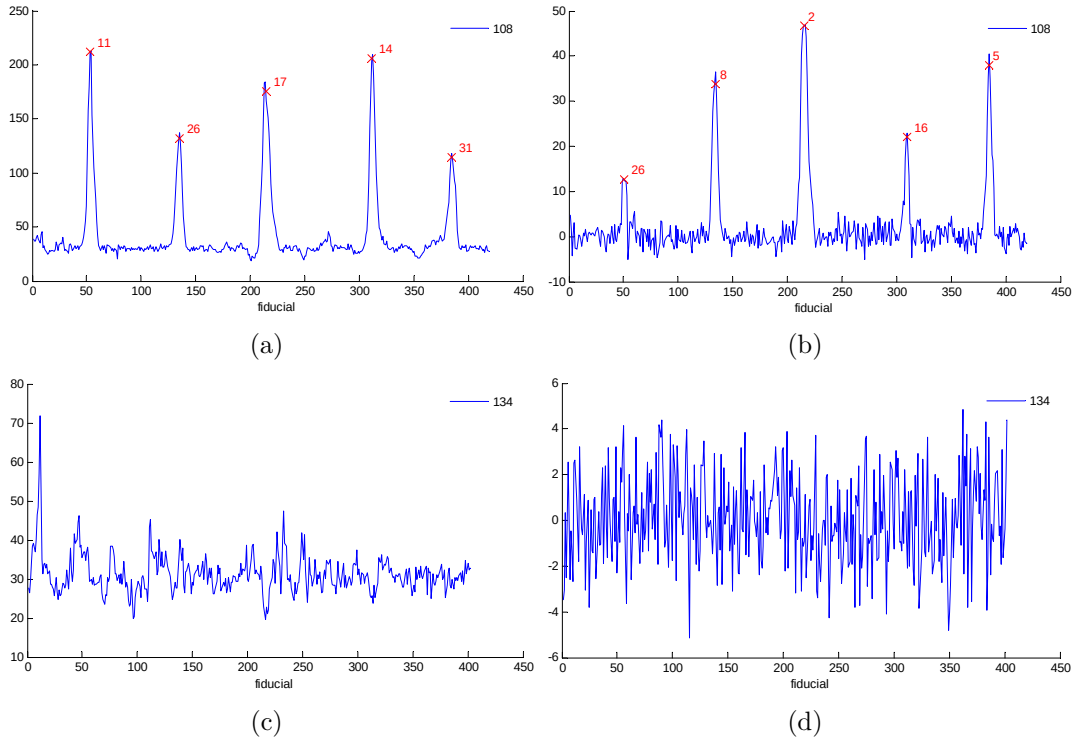

Figure 4.9. Example lines from one time gate before and after PCA. Units in mV. (a) Line including both UXO anomalies as well as cart orientation error. (b) Same line after PCA. Choosing a threshold from this line (8 mV) produced better anomaly picking results than from the non-PCA line. The numbers assigned to each peak are assigned by the autopicking routine, and thus change before and after PCA. (c) Example line that contains no UXO anomalies. Note the large anomaly due to orientation error. (d) Same line after PCA. No appreciable structure is present, and the magnitude is well below that of the UXO anomalies.

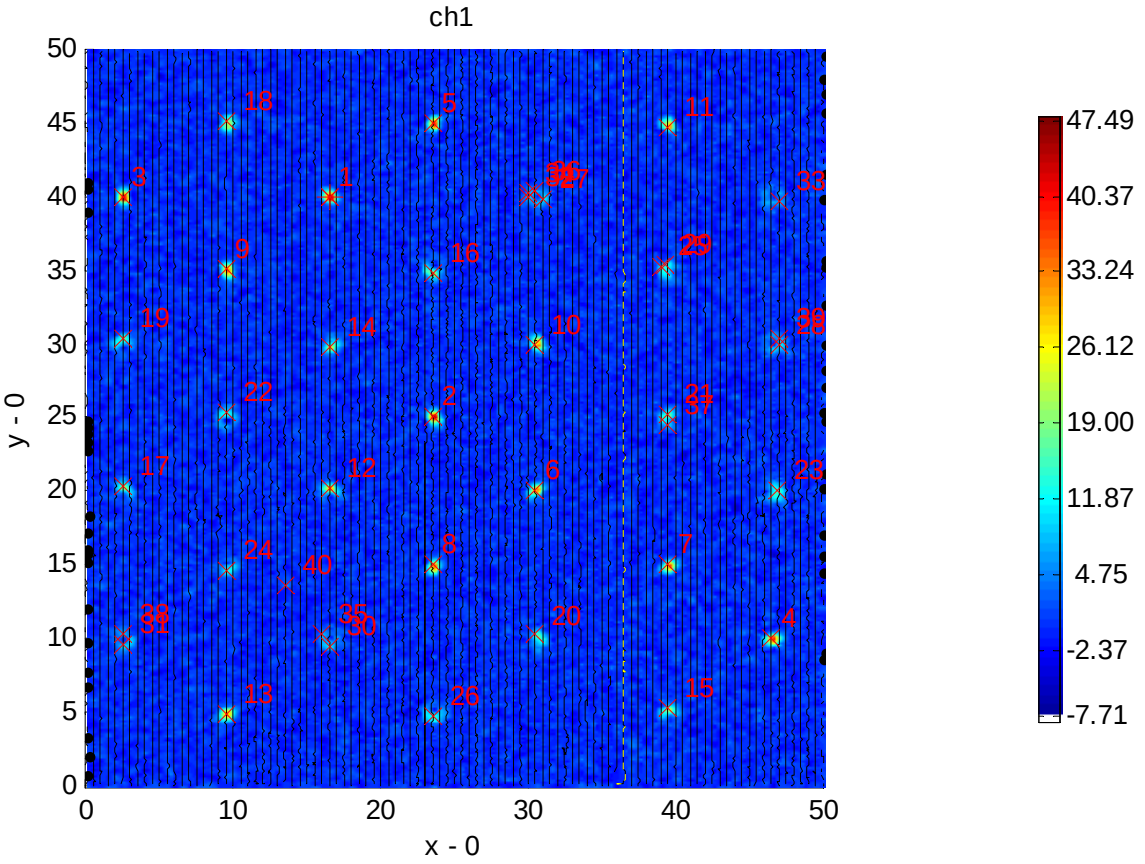

Figure 4.10. UXOLab anomaly picks after processing with PCA. After clustering, there was one false anomaly and no missed targets.

cessed dataset produced 32 picks, only one of which was false. There were no missed targets (Figure 4.10). This dataset is now ready for further processing via inversion of individual chosen anomalies or other methods. With standard techniques, these locations can be used on the original data for further processing. However, in order to incorporate PCA, UXOLab and other UXO toolboxes should be further developed to add rotation into their subsequent processing and inversion.

CHAPTER 5
SUMMARY

This is the final report for the SERDP project MM-1640 and it covers the research results accomplished since the inception of the project in 2007. The basic premise of this project is the theoretical understanding and algorithm development of principal component analysis as a denoising and signal-separation tool for transient electromagnetic (TEM) data in unexploded ordnance (UXO) applications. There is an express need for techniques to reduce the presence of random noise in TEM data as well as reduce the influence of correlated noise due to a wide variety of sources on automatic anomaly-picking routines for more accurate detection with fewer false anomalies. We have developed an algorithm and workflow for the processing and inversion of TEM data that attenuates signal from undesired sources and accurately inverts TEM data for diagnostic UXO parameters.

We separated the research in this project into aspects of PCA that address uncorrelated signals and aspects that address correlated but undesired signals, as well as interpretation of processed data. Specifically, these objectives included:

- Develop a PCA algorithm tailored to TEM data from UXO surveys, and
- Produce a stable and automated algorithm for removal of uncorrelated noise.
- Study the physical connection between signals due to different sources and the components recovered from PCA
- Determine the feasibility of using PCA to reduce TEM data in UXO applications to the signal exclusively produced by UXO and UXO-like anomalies, and
- Apply the developed algorithm to data examples and assess the effectiveness through discrimination/classification tests.

- Develop a method for parametric inversion of processed data for recovery of diagnostic parameters in UXO applications.

We have successfully accomplished these research goals over the course of the project.

Develop a PCA algorithm tailored to TEM data from UXO surveys

We developed an algorithm based on the Karhunen-Loéve transform tailored to UXO surveys by producing a temporally-correlated covariance matrix with proper data scaling. We have shown that this data organization and data scaling produces an effective algorithm for processing of UXO data. Spatially-correlated covariances investigate different characteristics of TEM data and are not immediately well-suited for UXO processing. In addition, spatial correlations require intensive numerical processing and significant user intervention in the process.

Produce a stable and automated algorithm for removal of uncorrelated noise

The PCA algorithm we developed reliably and automatically removes uncorrelated noise. Using an estimate of the error level in the data, the PCA algorithm automatically removes the proper principal components that contain the signal due to this uncorrelated noise. This is accomplished with a truncation matrix applied to the inverse rotation matrix that is defined by the number of eigenvalues required to reach the error level estimate. The processed data contain unaltered signal due to UXO with the random noise strongly attenuated.

Study the physical connection between signals due to different sources and the components recovered from PCA

Undesired signals in TEM surveys map into different principal components as a function of their decay characteristics. Both numerical simulation and field data

confirm that sources which contain static shifts, such as sensor orientation error and magnetic soils, map into the first principal component. These static sources tend to overlap with some of the signal produced by UXO; however, even with truncation of the first principal component, diagnostic decay and significant anomalies remain due to the UXO, and do not degrade performance of automated anomaly picking routines, such as those available in UXOLab. Sources which produce temporally-variant signals have much more variety in how they map into principal components, but tend to be well-separated from UXO and map into the 3rd and higher principal component.

Determine the feasibility of using PCA to reduce TEM data in UXO applications to the signal exclusively produced by UXO and UXO-like anomalies

We have determined through testing and experimentation of the algorithm on synthetic and field data that PCA can separate signals due to correlated noise from signals produced by UXO and UXO-like anomalies. We have also determined that the temporally-correlated PCA algorithm developed here is not appropriate for clutter analysis of individual anomalies when the entire dataset is processed at once. However, current research in SERDP and other projects suggests that various types of component analysis are effective in small, windowed areas for separating signals due to closely spaced targets.

Apply the developed algorithm to data examples and assess the effectiveness through discrimination/classification tests

We have successfully applied PCA to several synthetic and field datasets. In all cases, the signal-to-noise ratio was increased, the ability to detect anomalies in the presence of correlated noise was improved, and numerical inversion of individual anomalies of processed data was made possible.

Develop a method for parametric inversion of processed data for recovery of diagnostic parameters in UXO applications

Using the Pasion-Oldenburg model of the TEM response of UXO, we developed a method for parametric inversion of potential UXO targets for the investigation of diagnostic parameters. During the study, we discovered that data processed with PCA can not be inverted directly with the same forward model used to invert raw data. The forward model operator must incorporate the rotation and truncation matrices used in the PCA process. We have shown that by incorporating these matrices, the accuracy of the recovered diagnostic parameters can be improved.

In summary, MM-1640 has been successful in understanding the application of PCA in processing TEM data acquired for UXO applications. We have developed an algorithm ready for incorporation into standard UXO processing workflows for the improvement of detection of UXO and the reduction in false anomalies. We have also developed a consistent parametric inversion algorithm for PCA-processed data. The ability to identify and separate both random and correlated noise, and carry out parametric inversion using the processed data is expected to help improve the detection and discrimination ability and reduce the cost of UXO clearance.

ACKNOWLEDGMENTS

We would like to thank SERDP, Dr. Jeffrey Marqusee, Dr. Anne Andrews, Dr. Herb Nelson, Ms. Katherine Kaye, and Mr. Peter Knowles for funding and support. We also thank Len Pasion of the University of British Columbia for simulations and helpful discussions. We thank Trevor Irons and the rest of the Center for Gravity, Electrical, and Magnetic studies for support and assistance.

REFERENCES CITED

Asten, M., 2009, Use of principal component images for classification of the EM response of unexploded ordnance: Presented at the ASEG Annual Meeting.

Blackford, S., 2000, Hermitian eigenvalue problems, *in* Bai, Z., J. Demmel, J. Dongarra, A. Ruhe, and H. van der Vorst, eds., Templates for the Solution of Algebraic Eigenvalue Problems: A Practical Guide, SIAM.

Green, A., 1998, The use of multivariate statistical techniques for the analysis and display of AEM data: Exploration Geophysics, **29**, 77–82.

Hansen, P. C., 1992, Analysis of discrete ill-posed problems by means of the l-curve: SIAM Review, **34**, 561–580.

Hu, W., and L. Collins, 2004, Classification of closely spaced subsurface objects using electromagnetic induction data and blind source separation algorithms: Radio Science, **39**, RS4S07.

Hu, W., S. L. Tantum, and L. M. Collins, 2004, EMI-based classification of multiple closely spaced subsurface objects via independent component analysis: IEEE Transactions on Geoscience and Remote Sensing, **42**, 2544–2554.

Jackson, G., I. Mason, and S. Greenhalgh, 1991, Principal component transforms of triaxial recordings by singular value decomposition: Geophysics, **56**, 528–533.

Jones, I., and S. Levy, 1987, Signal-to-noise ratio enhancement in multichannel seismic data via the Karhunen-Loéve transform: Geophysical Prospecting, **35**, 12–32.

Kramer, H., and M. Mathews, 1956, A linear coding for transmitting a set of correlated signals: IRE Transactions on Information Theory, **IT-2**, 41–46.

Minty, B., and J. Hovgaard, 2002, Reducing noise in gamma-ray spectrometry using spectral component analysis: Exploration Geophysics, **33**, 172–176.

Minty, B., and P. McFadden, 1998, Improved NASVD smoothing of airborne gamma-ray spectra: Exploration Geophysics, **29**, 516–523.

Oldenburg, D. W., and Y. Li, 2005, Near-surface geophysics, chapter Inversion for applied geophysics: a tutorial. SEG.

Pasion, L., S. Billings, and D. Oldenburg, 2002, Evaluating the effects of magnetic susceptibility in UXO discrimination problems: Presented at the SAGEEP.

Pasion, L., and D. Oldenburg, 2001a, A discrimination algorithm for uxo using time domain electromagnetics: Journal of Environmental and Engineering Geophysics, **6**, 91.

———, 2001b, Locating and characterizing unexploded ordnance using time domain electromagnetic induction: Presented at the ERDC/GSL TR-01-10: USACE.

Rose-Pehrsson, S. L., R. E. Shaffer, J. R. McDonald, H. H. Nelson, R. E. Grimm, and T. A. Sprott, 1998, UXO target detection using magnetometry and EM survey data: Presented at the Proc. SPIE 3534.

Throckmorton, C. S., S. L. Tantum, Y. Tan, and L. M. Collins, 2007, Independent component analysis for UXO detection in highly cluttered environments: Journal of Applied Geophysics, **61**, 204–317.

UXOLab 2009, UXOLab: UXO detection and discrimination software, version 1.2.01. UBC-Geophysical Inversion Facility, Department of Earth and Ocean Sciences, University of British Columbia, Vancouver, British Columbia, Canada.

APPENDIX A
PUBLICATIONS AND PRESENTATIONS

Kass, M.A., and Y. Li, 2010, Quantitative analysis and interpretation of transient electromagnetic data via principal component analysis: Manuscript in preparation for submission to IEEE Journal of Geoscience and Remote Sensing.

Kass, M.A., Li, Y., and M. Nabighian, 2009, Enhancement of TEM data and noise characterization by principal component analysis: SERDP Symposium, Washington D.C.

Kass, M.A., Irons, T., and Y. Li, 2009, Inversion of multi-channel data with rotated kernels: 79th SEG International Meeting, Expanded Abstracts 28.

Kass, M.A., and Y. Li, 2009, Enhancement of transient electromagnetic data using principal component analysis: UXO/Countermine/Range Forum, Orlando, FL.

Kass, M.A., and Y. Li, 2007, Use of principal component analysis in the de-noising and signal separation of transient electromagnetic data: Presented at the 3rd International Conference on Environmental and Engineering Geophysics (ICEEG), Wuhan, China.